AD-A227 576

Annual Progress Report

for

Joint Services Electronics Program

Contract N00014-87-K-0327

for the period

10 October 1989 through 9 October 1990

G.L. Report No. 4738

Edward L. Ginzton Laboratory
Stanford University
Stanford, CA 94305

For the Faculty of the Edward L. Ginzton Laboratory
Professor S. E. Harris
Director

October 1990

90 10 10 126

Table of Contents

<u>Work Unit 90-1</u>   Development of an All-Silicon Integrated Optical
Modulator for High Speed Data Communications
(Professor D. M. Bloom)

<u>Work Unit 90-2</u>   Synthetic Nonlinear Media
(Professor R. L. Byer)

<u>Work Unit 90-3</u>   Scanning Tunneling Microscopy
(Professor C. F. Quate)

<u>Work Unit 90-4</u>   Device Related Properties of High-temperature
Superconductors
(Professor A. Kapitulnik)

<u>Appendix: Biography of Principal Investigators:</u>

Report Appendix
Bound Reprints, citing JSEP Sponsorship, under separate cover

Section I

Introduction

This is the annual progress report for the JSEP Program of the Edward L. Ginzton Laboratory at Stanford University for the period 9 October 1989 through 9 October 1990. This is the final report of the three-year unit. Since much of the material was covered in the recent proposal I will be somewhat brief.

During this period the research activities were organized into four work units:

Work Unit 90-1 — Development of an All-Silicon Integrated Optical Modulator for High Speed Data Communications (Professor D. M. Bloom)

Work Unit 90-2 — Synthetic Nonlinear Media (Professor R. L. Byer)

Work Unit 90-3 — Scanning Tunneling Microscopy and (Professor C. F. Quate).

Work Unit 90-4 — Device Related Properties of High-temperature Superconductors (R =)

I remark, as I did last year, that each of the above areas of research are based on innovative techniques that have been invented and developed in the Ginzton Laboratory. Taken together these different work units interconnect the physics and technology of linear and nonlinear materials and of optical fibers with new measurement tools, which provide unprecedented spatial and temporal resolution.

A very brief summary of some of the accomplishments of this Program follow:

Several years ago Professor David Bloom proposed a new type of optical modulator which is based on the phase interf- -ence which results from the variation of carrier density in pure silicon. During this previous year he has developed techniques for directly coupling this modulator to a single-mode optical fiber and has characterized this modulator in an all-fiber system.

The work of Professors Byer and Fejer has been particularly successful during this previous year. 0.15mW of single-mode power at 410 nm has been generated in a new type of

1

nonlinear media by periodically reversing the ferroelectric domains of lithium niobate. This work makes use of a unique lithographically patterned dopant technique. In the second area of work what are perhaps the largest nonlinearities that have ever been measured are obtained in GaAs quantum wells.

The work of Professor Quate and his students has led over the last several years to new techniques for forming atomic force microscope cantilevers and tips and entire microscopes on a single chip. The potential of this work both for reading and writing remains extraordinary. The Stanford group was invited to prepare the logo for STM '90. This logo was distributed on the conference letterhead.

Professor Kapitulnik continues to contribute to the understanding of high Tc superconductors. He developed techniques which allow materials with excellent superconducting properties to be readily grown. He also continues work on novel photothermal techniques, developed together with Professor Gordon Kino and which use Kino's confocal microscope, developed earlier on this Program.

This report also concludes the directorship of Professor S. E. Harris of the Edward L. Ginzton Laboratory portion of the Joint Services Electronics Program. Professor David Bloom will be the director for the next three year period.

Work Unit 90-1

Development of an All-Silicon Integrated Optical Modulator

for High Speed Data Communications

D. M. Bloom

(415) 723-0464

A. INTRODUCTION

Work during this reporting period has focused on the completion of two new developments of the all-silicon integrated light modulator. A modulator designed for push-pull operation has been fabricated and characterized. The expected doubling of modulation depth with no noise penalty was confirmed. Further a method for direct coupling of an optical fiber pigtail to a single side modulator has been developed, and this pigtailed modulator has been characterized in an all-fiber system.

B. SUMMARY OF PRINCIPAL ACCOMPLISHMENTS

We have completed the following work:

1. Development of a second generation all-silicon integrated modulator designed for push-pull operation. Measurements on this modulator show a doubling of the modulation depth compared to a design with only one active side.

2. Development of a technique for direct coupling of the silicon modulator to a single mode optical fiber and characterization of the this modulator in an all-fiber system. Modified for direct coupling to a single mode fiber, the modulator has a contrast of approximately 2:1 in a 60 MHz bandwidth.

C. DISCUSSION

1. Push-Pull Modulator:

In the first generation of the silicon modulator, one half of the optical beam was phase modulated while the other half acted only as a reference. By phase modulating the the formerly passive half of the beam an equal amount, but in exact opposite phase, we can double the total relative phase modulation between the two beams. In the linear region of the modulation curve, this gives twice the intensity modulation. This central idea behind the push-pull modulator is illustrated in figure 1.

Work to demonstrate this effect was started in the previous reporting period and completed during this period. After some initial processing problems were solved, the expected doubling of the modulation depth was demonstrated without any significant noise increase, i.e. the signal-to-noise was increased by close to 3 dB. A further advantage of the push-pull design is the reduced thermal parasitic signals at low frequency due to more symmetric power consumption in this design.

With this work B.R. Hemenway completed his Doctor of Philosophy degree in the Department of Applied Physics, Stanford University. He is presently working at Massachusetts Institute of Technology, Lincoln Laboratory.

2. Direct fiber coupling of silicon modulator:

The goal of the silicon light modulator project is to develop an interface between silicon integrated circuits and fiber optic communications. Compatibility with silicon integrated circuits has been demonstrated, and to show that he modulator is also compatible with fiber optics, we developed a simple, robust, low loss fiber to modulator coupling.

Because of the vertical structure of the modulator and the fact that there is no waveguide to couple into, the fiber to modulator coupling is effected by simply placing the fiber in direct contact with the back of the silicon chip. A schematic of the coupling is shown in figure 2. The light beam propagates unguided through the silicon and is reflected from the modulator back into the same fiber. To minimize the insertion loss due to the diffraction of the of the unguided beam, the total propagation length must be shorter than the Rayleigh length of the fiber optical mode, which in silicon is about 260 μm for 1.3 μm
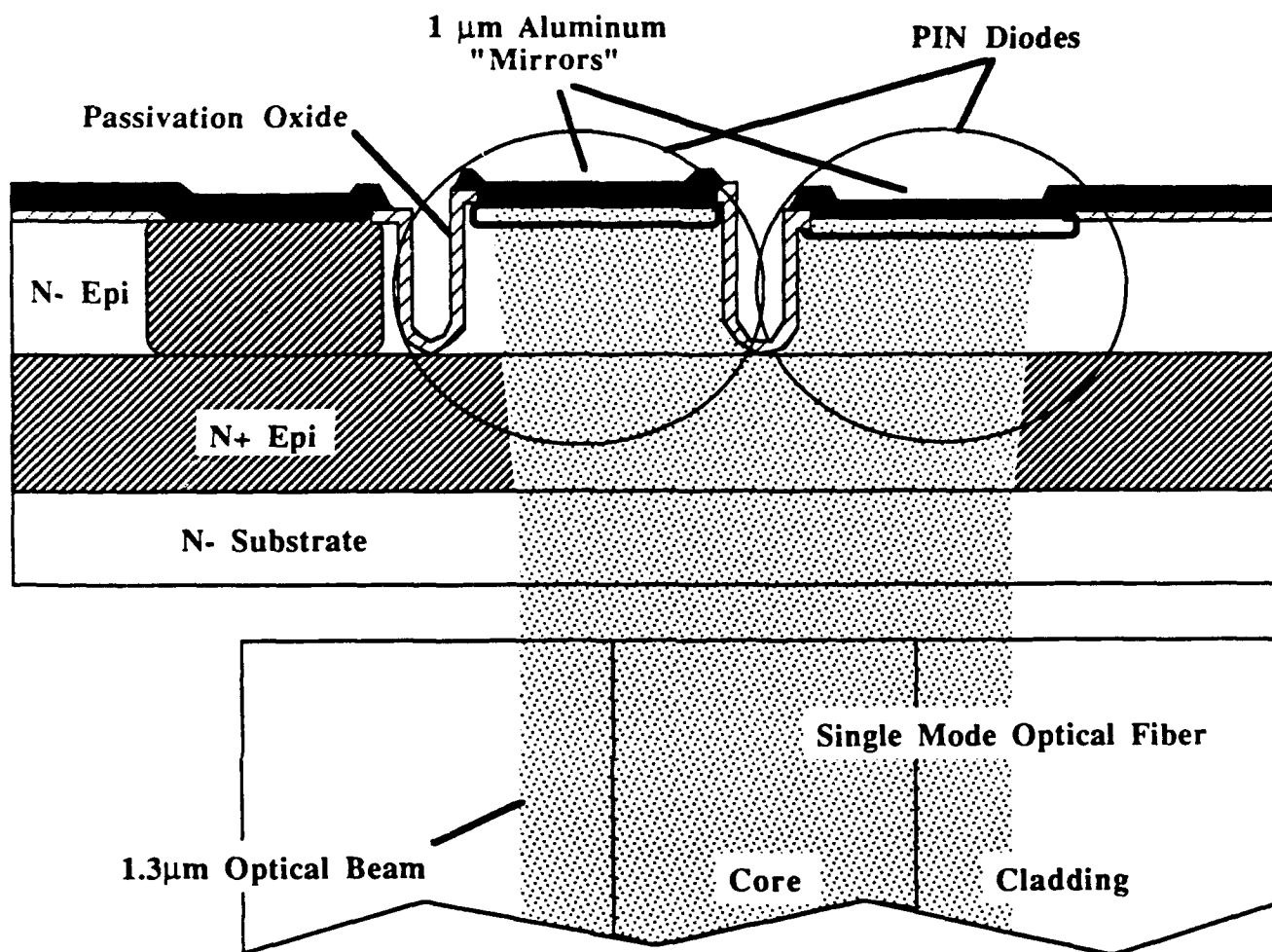
4

Figure 1. The figure shows a schematic cross section of the push-pull modulator. The two P-i-N diodes are driven in opposite phase, to produce twice the relative phase modulation of a modulator with one passive reference side. This cross section show the plasma etched trench that isolates the two P-i-N diodes. With high impedance drive circuitry, this trench is not necessary.

Epoxy filled chip carrier

UV curable epoxy

Silicon chip with modulator
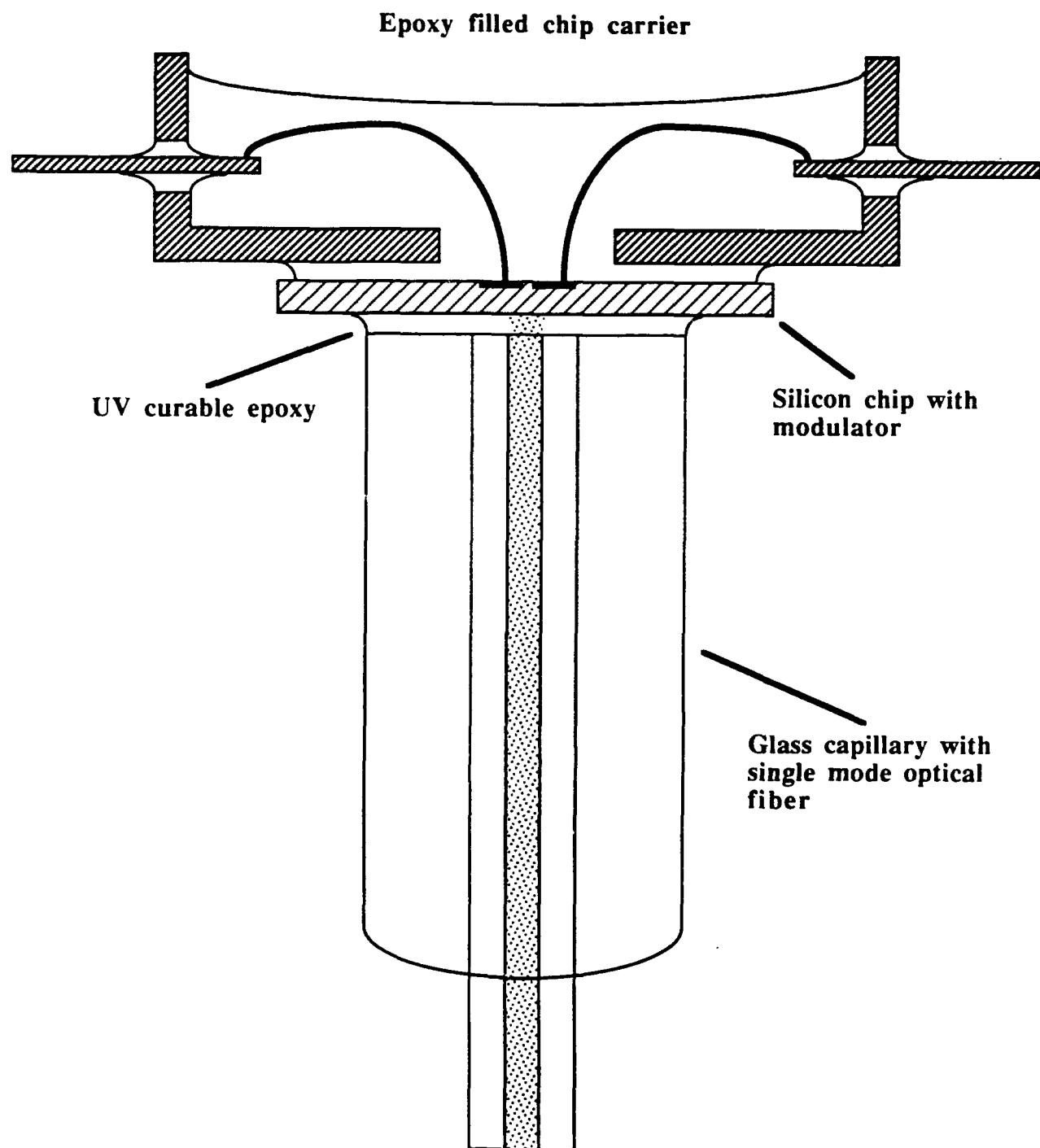
Glass capillary with single mode optical fiber

Figure 2. Schematic of modulator/fiber pigtail assembly. The fiber in the capillary is glued directly to the back of the thinned silicon chip. Electrical contact to the modulator is provided by the bond wires going through the hole in the bottom of the chip holder. the holder is filled with epoxy for rigidity.

light out of a 9/125 single mode fiber. The thickness of the silicon wafers is about 400 μm, showing that some thinning is necessary. We polished the chips down to a thickness of 50 μm, which leads to a diffraction loss of only 0.4 dB.

The fiber is placed in a glass capillary and this assembly is polished to produce a clean fiber termination that is sturdy enough to be handled by positioning tools. The thinned silicon chip is glued face down to the back of a chip holder. Electrical connection to the modulator is provided by bond wires going through a hole in the chip holder. For rigidity the holder is filled with epoxy. A rough alignment of the fiber and modulator is accomplished by launching light on the fiber and observing the spot on the front side of the modulator through a microscope using a infrared sensitive camera. With a signal input to the modulator, a final alignment is done to maximize the modulated output, before the fiber is glued in place using ultra violet curable epoxy.

The modulators used for direct fiber coupling had an area of 10 by 10 μm, roughly matching the mode size of the single mode fiber. The trench in the center of the modulator is approximately 1.5 μm wide. In this geometry the alignment tolerances are not very strict. Moving the fiber 1 μm relative to the fiber does not significantly alter the modulated signal. This displacement is larger than the shift in position due to curing of the epoxy, making this process uncritical. The resulting package after curing of the epoxy is extremely robust, with the weakest point being the the fiber itself at the point where it enters the capillary.

The pigtailed modulator was tested in the all-fiber system shown in figure 3. Here the source, the receiver and the power splitter all had fiber pigtails. A passive 3 dB power splitter was used to make the test system polarization independent. In this system the insertion loss was measured to be 5 dB, including two passes through a Photometric single mode reusable splice. To find the insertion loss for the light that is actually coupled out of the fiber, the effect of the light reflected from the glass/silicon interface must be considered. Without an anti reflection coating, roughly 15 % of the light will be reflected at this interface. Multiple reflections inside the silicon have high losses, so the light propagating on the fiber can be viewed as the result of only two interfering beams. The 5 dB insertion loss was measured with the temperature of the silicon chip adjusted to have the two beams interfering constructively.

When the two beams interfere destructively, the insertion loss is very high, meaning that the light intensity reflected from the modulator is comparable to the intensity reflected at the glass/silicon interface. The loss for the part of the beam that actually enters the modulator must then be in the 6 to 7 dB range. Roughly 3 dB is due to the optical bias
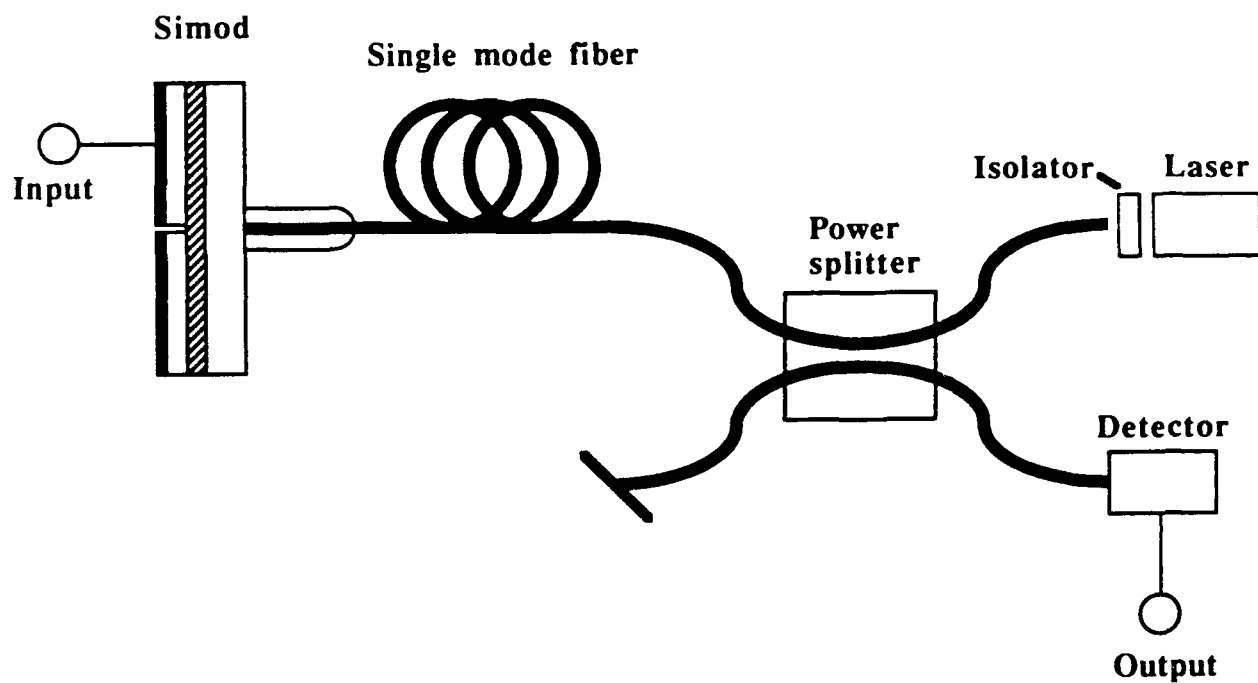
Figure 3.   All-fiber system for testing and characterization of the pigtailed silicon
modulator. The power splitter a passive polarization independent 3 dB
splitter, allowing measurements of the polarization dependence of the
modulator.

while only 0.4 dB is due to diffraction, as mentioned above. The additional loss is due to the trench in the middle of the device, poor reflectivity of the Al mirrors and bad alignment of the fiber. The absorption in the silicon is negligible.

The modulation depth of the modulator was 24 % with a 3 dB point at 60 MHz when driven with 30 mA DC current and an AC current of 60 mA peak to peak, meaning that the modulator is forward biased throughout the whole cycle. The bandwidth of the modulator is primarily determined by the lifetime of the carriers. Effects of the light reflected from the fiber/silicon interface discussed above influence the measured modulation depth. Because the measured modulation depth includes the unmodulated light reflected at the fiber/silicon interface, the light that actually couples into the silicon has a higher modulation depth than the measured value. With the two beams being of comparable magnitude, and the modulation depth being small, the intrinsic modulation depth is close to twice the measured value. With an anti reflection coating on the fiber/silicon interface we therefore expect a modulation depth of 50 % or a contrast of 2:1.

The polarization of the light in optical fibers changes with fiber stress and temperature. It is therefore an important advantage for fiber optic components to have a low polarization dependency. The measured polarization dependence of the modulator is only 0.55 dB, which is significantly lower than for most other types of fiber optic modulators.

With a distributed feedback semiconductor laser as the source, the noise in system was dominated by excess laser noise caused by optical feedback into the laser cavity. This was the case in spite of the fact that the laser was followed by an isolator providing 35 dB of optical isolation. A feedback insensitive source like a light emitting diode, super luminescent diode or ring cavity solid state laser would be preferable to a semiconductor laser in systems using this type of reflection modulator. We obtained the best signal-to-noise using a non-planar ring Nd-YAG laser. With this source we configured the all fiber system as an analog link and demonstrated good quality VHF video signal transmission.

D. PUBLICATIONS CITING JSEP SPONSORSHIP

B.R. Hemenway, O. Solgaard, A. A. Godil, D.M. Bloom, "A Polarization-independent Silicon Light Intensity Modulator for 1.32 μm Fiber Optics", IEEE Photonics Technology Letters, vol. 2, April 1990, pp. 262-264.

O. Solgaard, A.A. Godil, B.R. Hemenway, D.M. Bloom, "Pigtailed Single Mode Fiber Optic Modulator in Silicon.", accepted for publication in IEEE Photonics Letters.

REFERENCES

B.R. Hemenway, "Integrated Silicon Light Modulator for Fiber-Optic Interconnects at 1.3 Micron Wavelength", Edward L. Ginzton Laboratory Report # 4703, Doctor of Philosophy dissertation, Department of Applied Physics, Stanford University, May 1990.

B.R. Hemenway, O. Solgaard, D.M. Bloom, "All-silicon integrated optical modulator for 1.3 μm fiber-optic interconnects", Appl. Phys. Lett. 55 (4), 24 July 1989, pp.349-350.

B.R. Hemenway, O. Solgaard, A. A. Godil, D.M. Bloom, "A Polarization-independent Silicon Light Intensity Modulator for 1.32 μm Fiber Optics", IEEE Photonics Technology Letters, vol. 2, April 1990, pp. 262-264.

O. Solgaard, A.A. Godil, B.R. Hemenway, D.M. Bloom, "Pigtailed Single Mode Fiber Optic Modulator in Silicon.", accepted for publication in IEEE Photonics Letters.

<u>Work Unit 90-2</u>

SYNTHETIC NONLINEAR MEDIA

R. L. Byer
(415) 723-0226

A. INTRODUCTION

The goal of this project is the development of materials and device technologies suitable for efficient solid-state sources of coherent optical radiation. The difficulty in building laser diodes for the visible and mid-infrared motivates our interest in nonlinear frequency conversion devices able to convert available near-infrared laser diodes to other parts of the spectrum. Numerous applications exist for such devices, for example, a blue source for high storage density optical memories, xerographic processes and biomedical instrumentation, and coherent room-temperature mid-infrared sources for a variety of sensors and for the detection of industrial emissions or chemical agents.

Our work in this field is motivated in large part by improved diode lasers and diode-pumped lasers that have made it possible to commercially obtain hundreds of milliwatts of coherent output, and advances in materials technology that make it possible to tailor known materials in new ways and to design entirely new types of media. Emphasis is placed on techniques for laterally patterning the nonlinear properties of crystalline films for applications in waveguide devices.

This report covers both patterned media for nonlinear optical devices and fabrication and spectroscopy of thin polysilane films. The latter work is nearing completion, while the former forms the basis for the proposed 1991-1993 project as the transition from R. L. Byer to M. M. Fejer as principal investigator is completed.

B. SUMMARY OF PRINCIPAL ACCOMPLISHMENTS

The principal accomplishments of this work unit were:

1)   **Generation of coherent blue radiation** by quasi-phase-matched frequency doubling of the output of an infrared laser. Over 0.15 mW of single-mode power at 410 nm was generated in proton-exchanged waveguides fabricated in a lithium niobate substrate with **periodically reversed ferroelectric domains** created by indiffusion of a lithographically patterned dopant.

2) Measurement of **nonlinear susceptibilities** at 10.6 μm in excess of **10^{-7} m/V (1000 x bulk GaAs)** in three-layer asymmetric quantum wells, and **spatial patterning** of the suceptibility through proton-implantation-induced damage.

3) **VUV characterization of polysilane films** resolving the electronic structure responsible for the visible and UV linear and nonlinear responses.

C. DISCUSSION

In the patterned media project, both periodic ferroelectric domains in oxide crystals and laterally patterned semiconductor films have been studied. In both cases, the goal is to demonstrate efficient, compact and manufacturable nonlinear frequency conversion devices for applications like coherent blue light for optical storage and cell sorting, tunable infrared radiation for sensors, and parametric amplifiers for communications. The utility of patterning in these devices is for quasi-phase-matching (QPM), i.e. periodic modulation of the nonlinear properties of the medium at an integral multiple of the coherence length of the desired interaction. Through the use of QPM, one solves in a general way the fundamental materials problem in low power frequency conversion devices, finding a medium with adequate nonlinearity and transparency that can be phasematched for interactions of interest.

1. Periodic ferroelectric domains

Last year's report described the first application of periodically reversed ferroelectric domains to the generation of visible light by quasi-phase-matched waveguide second harmonic generation. As there described, the periodic reversals in the sign of the nonlinear coefficient that accompany such domain inversions allow QPM throughout the transparency range of lithium niobate, (0.35 μm – 4 μm). We investigated both planar and bulk devices. In the case of planar devices, the domain reversal was accomplished through indiffusion of a lithographically patterned dopant into standard commercially available substrates, while periodically-poled bulk crystals were grown by inducing compositional striations by periodically perturbing the temperature field in the growing crystal. Output power in the blue of up to 1 μW was reported in devices 1 mm in length.[1] The focus of the work in the current reporting year has been extension of these results to higher powers and longer devices.

The second harmonic generation efficiency of these devices can be described by

$$P_{2\omega}/P_{\omega} = \eta L_{eff}^2 P_{\omega} \qquad\qquad (1)$$

where $P_{2\omega}$ and P_{ω} are powers at the second harmonic and the fundamental, respectively, L_{eff} is the effective length of the device, and η is the normalized conversion efficiency [%/W-mm^2]. For SHG of blue light, with typical waveguide parameters, the theoretical value for η is 3.5%/mW-cm^2 for first order QPM (doman reversal every coherence length), and 0.35%/mW-mm^2 for third order QPM (domain reversal every three coherence lengths), but is often reduced by poor modal overlap or reduction of the nonlinear susceptibility during the waveguide fabrication process. L_{eff} is ideally equal to the physical length of the waveguide, but can be less if inhomogeneities spoil the phasematching. P_{ω} is ultimately limited by the available sources (typically 100 - 200 mW for commercial single-mode laser diodes), but can be less if the waveguide damages at a lower power. From these figures we see that ideally 35% conversion effciency can be obtained with 10 mW input in a first order device or with 100 mW in a third order device.

From the previous discussion, three quantities can be identified that completely describe the quality of the device, η, L_{eff}, and P_{ω}. The devices reported last year were third order, and had η = 40%/W-cm^2, $L_{eff} = L = 1$ mm, $P_{\omega} = 15$ mW (source limited), producing 1 µW of blue light. While the normalized conversion efficiency was nearly an order of magnitude smaller than theoretical, it was still large enough that > 1 mW of output was anticipated for 50 mW of input in a device scaled to 1 cm in length. After construction of such devices, it was found that the effective length was only 2 - 3 mm, indicating that inhomogeneities in the waveguide were limiting the phasematchable length.

From the preceding, three important issues arise: improving the normalized efficiency, increasing the phasematchable length, and increasing the in-coupled fundamental power. Improved sources and coupling efficiency (total insertion losses are now $\approx$ 3 dB for 1 cm long devices) have allowed us to couple as much as 140 mW infrared input into the waveguide, resulting in as much as 150 µW of blue output power. This result is important both in that it is two orders of magnitude more output than possible last year, and because it shows the waveguides are capable of supporting powers as large as can be anticipated from diode sources.

The other two issues are more complex. The limited effective length results from variations in the waveguide dimensions, which, through the contribution of the waveguide

to the dispersion, lead to variations in the coherence length. An axially varying coherence length prevents a single grating period from QPM over the entire length of the device. The tolerance for such variations depends on the nature of their axial dependence, but is typically several percent. While this problem could be addressed by careful lithography of the waveguide channels, a more attractive approach is "non-critical phasematching." By choosing the waveguide dimensions appropriately, one can find an operating point at which the waveguide dispersion at the second harmonic exactly compensates that at the fundamental, so that there is no first order dependence of the dispersion on the waveguide dimensions. An experiment measuring the dispersion of ten proton exchanged waveguides of various depths agreed closely with this theoretical prediction. Waveguides operated at the noncritical point typically have tolerances increased an order of magnitude over critical operation. This concept is potentially very important, as it can be applied to any waveguide nonlinear interaction, including those phasematched by means other than QPM. A paper and a patent application describing this concept have been submitted, both acknowledging JSEP support.[2] To design a noncritical waveguide, good knowledge of the waveguide fabrication process is necessary, as discussed in the following.

The low value of η could be due either to poor overlap of the modes with the domain reversed region or to a reduction in the nonlinear susceptibility due to the waveguide fabrication process. Careful measurements of the mode shapes indicated that the former explanation was unlikely, so we believe the latter to be responsible. It is known that the proton exchange waveguide process can reduce the nonlinear susceptibility at high proton concentrations, so for our early devices we adopted an annealing step to reduce the concentration. However, the proton exchange process involves a highly nonlinear diffusion step and results in an index of refraction change that is also a highly nonlinear function of the proton concentration, and so is not as well understood as the simpler processes such as Ti indiffusion. To facilitate design of waveguides that are both noncritical and retain the full nonlinear coefficient, we have undertaken a detailed study of the annealed proton exchange process, and now have a workable model of the dispersion and mode depths over a useful parameter space. A noncritical design incorporating these data is now being fabricated. If, as we expect, it will have both a full 1 cm effective length and close to the theoretical normalized conversion efficiency, the output will be several milliwatts of blue radiation with a diode laser pump.

Progress continues in the growth of periodically-poled lithium niobate crystals, of interest for higher power interactions such as Nd laser pumped green and IR sources. As

discussed in last year's report, we have used our laser-heated-pedestal-growth apparatus to produce periodically-poled crystals of good optical quality, with domain spacings down to 1 μm, capable of supporting > 100 mW of 488 nm radiation, dramatically higher powers than possible in uniformly poled crystals.[3] The major issue to be resolved was the effective length of the crystals, limited to several hundred microns by random errors in the domain positions, as measured by the width of the phasematching curve for SHG of blue radiation. We have since improved our growth technology, and have produced crystals with domains coherent over > 2 mm lengths (1500 domains), with peaks 5 times narrower than those obtained last year, though an undesired periodic phase modulation of the domains remains a problem. This phase modulation is probably associated with a slow drift in the freezing interface during growth, an issue we are currently investigating. As another path to obtaining bulk periodically-poled crystals, we have been collaborating with Crystal Technology (Palo Alto, CA) on the development of a periodic poling process scaled up to cm diameter crystals, with promising results on crystals with long (30 μm) domains suited to IR interactions.

2. Patterned Semiconductor Films

While we are obtaining excellent results with periodically-poled lithium niobate deviecs, we are also pursuing other material systems amenable to lateral patterning. Such studies are of interest for two reasons. From a practical standpoint, the major cost associated with a diode-laser-pumped device in lithium niobate will be neither that of the diode laser nor that of the lithium niobate structure, both of which will cost several dollars to manufacture in quantity, but rather that of aligning and assembling the laser to the device with the requisite micron tolerances. A nonlinear medium that can be deposited on the same substrate as the laser can eliminate this cost, which has lead to studies of, for example, polymer films ("blue paint") and oxide ceramics (PLZT) for deposition on III-V substrates. An alternative, attractive from the materials growth standpoint, is a transparent wide-bandgap II-VI film grown epitaxially on the III-V substrate. From a fundamental standpoint, extension of efficient nonlinear frequency conversion into the infrared requires materials with good IR transparency and large nonlinearities. The nonlinear susceptibility typically decreases steeply with increasing bandgap, so that lithium niobate, with its absorption edge in the UV, is in some sense "too transparent" for optimal applicability in the IR, suggesting the use of "bulk" III-V films or quantum well devices with enhanced IR nonlinearities.

15

In last year's report we described the demonstration of extremely large mid-IR nonlinearities in electric-field-biased quantum wells. We have continued these studies, as well as initiating exploratory studies of patterned III-V films with the J. S. Harris group and II-VI films with the J. Gibbons and R. Feigelson groups.

The IR nonlinearities in III-V quantum wells are based on mid/far-infrared transitions between conduction subbands. These subband states can be accurately pictured as the "particle in a box" states familiar from basic quantum mechanics. Transitions between these subbands have large dipole matrix elements (oscillator strengths on the order of m_e/m^*, or 15 for GaAs), tunable energy differences typically resonant with 5 - 15 μm radiation, and narrow linewidths (the ground and excited subbands have approximately the same curvature). Together with the symmetry breaking introduced by applying a bias electric field or growing an asymmetric structure, these properties lead to a large infrared nonlinear susceptibility. Last year we reported second order suceptibilities 70 times larger than that of bulk GaAs observed in electric-field-biased AlGaAs wells, in good accord with theoretical predicitons.[4] We have since extended this work to asymmetric three layer step quantum wells. An absorption spectrum of this sample clearly showed both 1-2 and 1-3 transitions, the latter allowed only in asymmetric structures. The larger oscillator strength of the 1-3 transition compared to that in the electric-field biased wells leads to an order of magnitude increase in the nonlinear susceptibility, to 2×10^{-7} m/V, 1000 times larger than that of bulk GaAs. Another important step taken with these asymmetric wells was lateral patterning of the nonlinear susceptibility through proton implantation damage. By selectively eliminating the carriers with implantation through a mask, it was possible to completely eliminate the nonlinear susceptibility in the damaged regions without affecting the nonlinearity in the unimplanted regions. Combining this lateral patterning capability for QPM with the incorporation with quantum wells embedded in an epitaxially grown waveguide, and a novel surface emitting geometry[5], a project being pursued in collaboration with the J. S. Harris group, we predict efficiencies for mid-IR mixing experiments of >10% with 100 mW inputs.

We have also begun studies based on modulation of the bulk properties of epitaxially grown films. Also with the J. S. Harris group, we have grown films of alternating single crystal/disordered GaAs on a GaAs substrate. The random orientation of the disordered regions leads to zero effective nonlinearity, so that we again achieve control for QPM. In this case, the patterning is accomplished by growth on a substrate previously patterned with

an SiO_2 grating, the disordered material corresponding to that grown on the SiO_2. With the 6 x larger nonlinear coefficient of GaAs compared to $LiNbO_3$, one expects 36 x greater efficiency for a given interaction in GaAs. This is of interest both for IR mixing and for parametric amplification of communication wavelengths (1.3 and 1.5 μm), for the latter of which we predict single pass gains $\approx$ 1 dB/mW. For visible interactions, we have begun with the J. Gibbons group studies of films of II-VI crystals with periodically varying crystalline orientation. It has been observed that growth on certain nonpolar films leads to antiphase domains and growth on certain strained layers leads to regions of rotated orientation. By patterning the intermediate layer between the substrate and the waveguide film, we hope to induce such modulations periodically. If this technique works, it will be very powerful, as we will then have the ability to create a "template" on which a variety of materials compatible with GaAs can be grown with arbitrary patterning.

3. Polysilane films

Polysilane polymers consist of a long catenated σ-bonded silicon backbone with two sidegroups, usually carbon based, attached to each Si atom in the backbone chain. They are soluble in most hydrocarbon solvents and thin films of excellent optical quality can be fabricated with conventional spinning and coating techniques. In spite of the σ-bonded nature of the backbone, the polysilanes show extensive electronic delocalization, resulting in strong transitions for excitations polarized parallel to the backbone. This delocalization is responsible for the curious linear and nonlinear optical properties of these polymers, and leads to very large oscillator strengths for excitations polarized parallel to the backbone.[6] Excitations due to absorption of UV photons decay either by UV fluorescence or scission of the polymer backbone, making these materials useful as deep UV photoresists for microlithography. These large oscillator strengths also give rise to large optical nonlinear susceptibilities.

Our earlier work has concentrated on fabrication and characterization of polysilane films for use as waveguides. This work was carried out in collaboration with R.D. Miller and J. Zavislan of the IBM Almaden Research Center. It was found that correct choice of polymer molecular weight, solvent, and spinning conditions can produce thin films and waveguides. We also studied the nonlinear (two-photon) absorption properties of poly(di-n-hexylsilane). Two-photon exposure of this polymer produces anisotropic scission, making the exposed area highly birefringent.[7] This birefringence allows the realization of several unique optical devices, particularly for waveguide applications.[8] A spectrum of the

17

effect shows the process to be highly resonant for a two-photon energy of 4.3 eV, considerably higher than the single photon absorption, which occurs at 3.3 eV.

The nature of these two-photon transitions can only be understood in the context provided by the overall electronic structure of the polymer. This structure has been the subject of some debate. Some have predicted that the first UV absorption arises from a band-to-band transition, while others ascribe it to a tightly bound Frenkel-type exciton. We have therefore measured the VUV spectrum of the polysilane polymer poly(di-n-hexylsilane) in an attempt to clarify this question.

The measurements are taken using a reflection spectrometer, developed at DuPont laboratories. The complete reflectivity spectrum was measured from 0.5 to 44 eV (2.5 μm - 30 nm), and normalized to agree with known values of refractive index at visible wavelengths. The $\approx \omega^{-4}$ dependence of R at high energy indicates that all transitions between the valence and conduction band have been included, and that the optical properties can therefore be calculated through a standard Kramers-Kronig analysis.

The calculated value of the extinction coefficient, k, has been compared with a theoretical prediction of k from the first-principles band structure calculation of Mintmire for poly(di-methylsilane).[9] With the assignment of the direct gap of the polymer to the second UV absorption, the correspondence between the features predicted by the theory and determined by our measurement is quite good. The deviation at higher energy can be attributed to transitions in the hexyl sidegroups, not included in Mintmire's calculations. This spectrum allows us to suggest that the first UV absorption arises from the formation of an exciton, with a binding energy of $\approx$ 600 meV. This agrees quite well with theoretical predictions of the properties of excitons in quantum wires, assuming the 'wire' dimensions have been reduced to correspond to the physical dimensions of the polymer backbone.

Although we assign the direct gap to an energy lower than the two-photon transition, the highly allowed direct gap will be highly forbidden to two-photon transitions. It is therefore reasonable to also also assign the first two-photon absorption we observe to an exciton, bound to a higher energy band. Very fast nonlinear waveguide switching devices have been proposed using excitonic nonlinearities such as the nonlinear refractive index, n_2.[10] This is related to the two-photon absorption coefficient β through a Kramers-Kronig relation. The nonlinear susceptibility calculated in this way shows the characteristic

dispersion lineshapes expected from the two-photon absorption, and furthermore indicates that there is a spectral region with low two-photon absorption where the nonlinear index of refraction is significantly enhanced. This spectral region (640-700 nm) corresponds to a wavelength region where commercial diode lasers are available. Although these lasers are generally low power devices, when focussed into a waveguide with a few microns cross sectional area, the intensity can be high enough to drive several proposed nonlinear switching devices. The possibility of fast intensity modulation of these sources, combined with the high nonlinearity of the polysilane polymers and the ease of fabricating and patterning waveguides, suggests that the polysilanes may have utility in demonstrating integrated optical devices.

In this regard, Stegeman et al[11] have proposed a figure of merit $T=2\beta\lambda/n_2$ for a nonlinear directional coupler, with T values < 1 implying useful materials. In the case of poly(di-n-hexylsilane), our lower bound estimate on n_2 yields a T value ranging from 0.1 - 1.0 for the wavelength range 580-650 nm. Preliminary measurements using a prism coupler yield a repeatable shift in a waveguide mode corresponding to an n_2 value of $\approx 60 \times 10^{-6}$ (cm^2/MW), 4 times larger than that predicted by our lower bound estimate. However, spurious effects due to heating photoinduced birefringence, etc. at this time cannot be conclusively ruled out, and this result is presented only as a comparison to the theoretical value. Further measurements are necessary to confirm these preliminary results and determine the utility of the polysilanes for practical nonlinear optical devices.

REFERENCES

1 . E. J. Lim, M. M. Fejer, and R. L. Byer, "Second Harmonic Generation of Green Light in a Periodically-Poled Planar Lithium Niobate Waveguide," Electron. Lett. 25, 174-175 (1989).
E. J. Lim, M. M. Fejer, R. L. Byer, and W. J. Kozlovsky, "Blue light generation by frequency doubling in a periodically poled lithium niobate channel waveguide," Electron. Lett. 25, 731-732 (1989).

2. E. J. Lim, S. Matsumoto, and M. M. Fejer, "Noncritical phasematching for guided-wave frequency conversion," accepted to Appl. Phys. Lett..

3. G. A. Magel, M. M. Fejer, and R. L. Byer, "Quasi-phase-matched second harmonic generation of blue light in periodically-poled LiNbO3," Appl. Phys. Lett. 56, 108 – 110 (1990).

4. M. M. Fejer, S. J. B. Yoo, R. L. Byer, A. Harwit, and J. S. Harris, Jr., "Observation of Extremely Large Second Order Susceptibility at 9.6 – 10.8 μm in Electric-Field-Biased Quantum Wells," Phys. Rev. Lett. 62, 1041-44 (1989).

5. M. M. Fejer, "Second Order Nonlinearities in Asymmetric Quantum Wells," IQEC, Anaheim, 1990.

6. R.D. Miller and J. Michl, Chem. Rev. 89, 1359-1410 (1989)

7. F.M. Schellenberg, R.L. Byer, and R.D. Miller, Chem. Phys. Lett. 166, 331 (1989) and F.M. Schellenberg, R.L. Byer, R.D. Miller, and S. Kano, Mol. Cryst. Liq Cryst. 183, 197 (1990)

8. F.M. Schellenberg, patents pending; and F.M. Schellenberg, R.L. Byer, and R.D. Miller, Opt. Lett. 15, 242-244 (1990)

9. J.W. Mintmire, Phys. Rev. B 39, 13350 (1989)

10. See, for example, Optical Switching in Low Dimensional Systems, H. Haug and L. Banyai, eds., Plenum Press, New York (1989) or Nonlinear Optics of Organics and Semiconductors, T. Kobayashi, ed., Springer Verlag, Heidelberg (1989)

11. K.W. Delong, K.B. Rochford, and G.I. Stegeman, Appl. Phys. Lett 55, 1823 (1989)

D. PUBLICATIONS AND PATENTS CITING JSEP SPONSORSHIP

PUBLICATIONS

1. D. H. Jundt, M. M. Fejer, and R. L. Byer, "Characterization of single-crystal sapphire fibers for optical power delivery applications," *Appl. Phys. Lett.* 55, 2170 – 2172 (1989).

2. M. M. Fejer, G. A. Magel, and E. J. Lim, "Quasi-phase-matched interactions in lithium niobate," *Proc. SPIE* 1148, 213 – 224 (1989).

3. G. A. Magel, M. M. Fejer, and R. L. Byer, "Quasi-phase-matched second harmonic generation of blue light in periodically-poled LiNbO₃," *Appl. Phys. Lett.* 56, 108 – 110 (1990).

4. D. H. Jundt, M. M. Fejer, and R. L. Byer, "Optical properties of lithium-rich lithium niobate fabricated by vapor transport equilibration," *IEEE J. Quantum Electron.* 26, 135 – 138 (1990).

5. Dieter H. Jundt, Martin M. Fejer, and R. L. Byer, "Growth of optical quality single crystal sapphire fibers, *Mat. Res. Soc. Symp. Proc.* 172, 273 – 278 (1990).

6. E. J. Lim, S. Matsumoto, and M. M. Fejer, "Noncritical phasematching for guided-wave frequency conversion," accepted to *Appl. Phys. Lett.*.

Note that publications 1, 4 and 5 discuss work that is not presented in the 1990 Final Report but that was described in the 1988 Final Report .

PATENTS

1. G. A. Magel, M. M. Fejer, and R. L. Byer, "Method of Producing Monocrystalline Rods Having Regions of Reversed Dominant Ferroelectric Polarity and Method for Clarifying Such a Rod," pending.

2. E. J. Lim and M. M. Fejer, "Waveguide Phasematching," pending.

SCANNING TUNNELING MICROSCOPY

Calvin F. Quate

(415) 723-0213

A. INTRODUCTION

1. Integrated Systems (STM-on-a-chip, the AFM)

The project labeled "STM-on-a-chip" revolved around the fabrication of a Tunneling Microscope on a single silicon chip. This project has been successful and we now have wafers with numerous chips each containing an STM.

Our success in this program has inspired us to review the possibility of integrating other instruments with the technology of microfabrication. The Atomic Force Microscope (AFM) with an integrated tip and an integrated device for sensing the cantilever deflection is our current choice.

2. AFM Studies

(a) VLSI Metrology with the AFM

We are applying the atomic force microscope (AFM) to dimensional measurements of microfabricated structures. The AFM functions as a scaled-down stylus profilometer, scanning a sharpened tip across a surface and measuring the tip-sample forces to determine the surface topography. By scaling down the physical size of the probe and increasing the sensitivity of the detection system, the AFM achieves much higher resolution and much higher data collection rates than a profilometer. The AFM is more versatile than the scanning tunneling microscope for topographical measurements because insulating samples can be imaged and also because subtle electronic structure effects do not significantly alter the topographs. The AFM also improves upon the scanning electron microscope by providing true height information about the sample (i.e. film thicknesses),

instead of providing a two-dimensional projection of a three-dimensional sample. We are studying the practicality of making reliable dimensional measurements of microfabricated structures with the AFM.

(b) Charge Storage

It is well-known that the metal/silicon nitride/silicon dioxide/silicon system can be used for non-volatile memory applications.[1] By applying a bias between the metal and the silicon, charge can tunnel from the silicon, through the silicon dioxide, to be trapped in the silicon nitride. This charge induces a depletion region in the silicon which can be detected by the resulting change in capacitance between the metal and the silicon. Likewise, this charge can be untrapped by applying a reverse bias, restoring the system to its initial state. This charge can be trapped and untrapped many times and has a retention time on the order of years.

We have replaced the fixed metal contact with a flexible metal cantilever that can be scanned across the surface of the silicon nitride. This method allows a single probe to address individual "memory cells", with their size limited only by the probe size and the sensitivity of the capacitance detection electronics. Unlike other proposed storage systems using the STM or AFM, this method is much more robust because the information is stored beneath the surface of the storage medium, reducing the need to protect the surface. Also, this storage method is completely reversible, unlike lithography-based storage methods.

3. Nanometer-Scale Hole Formation on Graphite using an STM

Nanometer-scale surface modification and manipulation with the STM has been used to fabricate small structures on selected substrates. This technique has great potential for applications in areas such as high resolution lithography and high density storage. The small structures, with dimensions comparable to the wavelength of electrons, should exhibit interesting properties since the electronic behavior is dominated by quantum mechanics.

During this interval we have focused much of our attention on the chemical etching of holes in the uppermost layers of HOPG. It is a subject that we introduced in our annual report of 1989.

4. Gold on Gold Epitaxy

While epitaxial growth on semiconductors has received significant attention for its obvious technological interest, epitaxy on metal surfaces has been somewhat neglected. On semiconductors, STM proved a unique local non-averaging probe of the surface atomic structure. We successfully applied the technique to the study of a model metal-on-metal system, the (111) silver-gold interface.

Growth of the four possible overlayer-substrate combinations was observed under ultra-high vacuum conditions from its initial stages to the formation of several layers, leading to a unified understanding of the room-temperature growth in this system. Generally applicable techniques for the extraction of quantitative information, such as cluster size distributions and spatial correlation functions, from the STM images were developed.

Furthermore, we examined the evolution of the surface topography of the Au(111) surface during ion bombardement. While sputtering theory could never before be checked on the microscopic scale, this work also establishes an unexpected beautiful link to the epitaxy studies.

B. SUMMARY OF PRINCIPAL ACCOMPLISHMENTS

1. Integrated Systems (STM-on-a-chip, the AFM)

Our microfabrication work has yielded devices of two basic types: entire microscopes on chips, and AFM cantilevers and tips. The original microfabricated AFM cantilevers were made of silicon dioxide with no protruding tip. We now have the capability of fabricating cantilevers of many materials including silicon, silicon dioxide, silicon nitride and metals. In addition, we have developed an assortment of tips which can be integrally

fabricated on these cantilevers. Our preferred AFM cantilever is made of silicon nitride with a sharp, single crystal silicon tip. The silicon nitride cantilevers are much more rugged than silicon, or silicon dioxide, cantilevers. The silicon tips are self-sharpened by an oxidation step during fabrication. The tips, with a reproducible shape, have a radii of curvature of approximately 200 Å. The robustness of this assembly was demonstrated by imaging an integrated circuit with the repulsive mode at x-scan rates of 1200 Hz while scanning over a range of 15 microns.

The microfabrication of entire microscopes on silicon chips was first demonstrated in our group and successfully used to image atomic structure. We are currently developing an AFM counterpart which consists of a silicon cantilever with strain sensitive devices built as an integral part of the cantilever. Preliminary experiments indicate that sub-nanometer vertical resolution can be achieved. We believe that the new AFM chip will have applications ranging from contact profilometry to UHV surface studies and to sensing elements in electronic devices. We are working on two approaches: (1) a piezoelectric film on a nitride cantilever, and (2) a piezoresistive element built into a silicon cantilever.

The piezo-films are the ZnO films that were fabricated in connection with the STM-on-a-chip. The films were originally designed to be voltage driven for the purpose of moving the cantilever. We now believe that they can be used for sensing. In our preliminary work we found that deflection of the cantilever does indeed produce an electrical response in the piezo-film, but the sensitivity is not yet good enough. We can detect a motion of 10 Å in the cantilever which compares with the 1 Å that is required for most of the applications that we envision.

The piezoresistive elements are based on piezoresistive effect in silicon where an applied stress will change the resistance of the semiconductor. The miniature sensor is made by integrating a resistor into a silicon cantilever beam. It should be possible to monitor beam deflections by monitoring changes in the value of that resistor. Three other

25

balancing resistors which connect to the sensor in a bridge circuit are built on the same chip.

Design specifications have been selected to meet the requirements for using the device as a sensor for atomic force microscopy. Those specifications include a sensitivity of 1 Å in the measurement of the displacement, a spring constant of the cantilever of about 1 N/m and ease of approaching a sample to the cantilever.

Four wafers have been processed and their electrical characteristics have been tested. Although the performances are affected by incomplete activation of the carriers during anneal and leakage in shallow, heavily doped junctions, the devices have the expected characteristics.

2. AFM Studies

(a) VLSI Metrology with the AFM

The two critical components of the AFM for this application are the scanner and the cantilever. We have worked to optimize these components for this application. We constructed a 1" long piezoelectric scanner that has an 18 μm scan range and a lowest resonance frequency of about 2 kHz. This scanner allows us to image complete microfabricated structures at high speeds. We have also microfabricated silicon nitride cantilevers with integral single-crystal silicon tips that have a narrow apex angle and a small tip radius-of-curvature. These tips allow us to image near tall structures and into deep trenches with a minimum of tip-induced artifacts. They are also rugged enough to allow high-speed imaging of hard samples without damage.

We have imaged several microfabricated structures with the AFM. These include glass and silicon gratings, closely-spaced "dot" patterns, optical linewidth standards, PMMA-on-Si films that have been patterned by projection x-ray lithography, and a GaAs MESFET. These images allow us to evaluate the AFM as a dimensional measurement instrument. We have also increased the imaging rate of our AFM to several frames per

second which provides nearly instantaneous feedback for operator adjustments. This high-speed imaging greatly increases the utility of the AFM for routine measurements.

(b) Charge Storage

We have fabricated nitride/oxide/silicon wafers in order to test the charge storage mechanism. Bulk devices were made by depositing metal on these wafers, and they were found to exhibit the expected variations of capacitance, though with a retention time of hours instead of years. This is attributed to a thinner than desired oxide film that allows the trapped charge to tunnel back out of the nitride into the silicon. After this initial success, we installed a capacitance sensor on our AFM and began a study of laterally resolved charge trapping and capacitive imaging. Using etched wire cantilevers, we have been able to form and image charge-trapped regions as small as 2000 Å. This writing process is repeatable and erasable. We have written patterns of charge "dots", imaged them, and been able to erase individual dots from the pattern. The amount of charge that is stored for a given dot is also controllable and results in a corresponding shift in the flat-band voltage of the MOS capacitor. We have obtained flat-band voltage shifts of up to 10V using this method.

3. Nanometer-Scale Hole Formation on Graphite using an STM

Our work on writing with holes in graphite caught the attention of the people organizing the international conference on tunneling microscopy - STM '90 and NANO I - held in Baltimore, Maryland, July 1990. We were invited to prepare a logo for this conference written with the small scale dots on graphite. This logo appeared as part of the letterhead on the official conference stationary.

A more important accomplishment is the work that has allowed us to gain some understanding of this phenomena. It was evident early on that the surface pits would not appear if the graphite was placed in vacuum; a vapor of water molecules was needed. The formation of pits controlled by the position of the tip is a form of etching, enhanced by the tunneling electrons.

The experimental work at Stanford has been extended by collaborative work with N.S. Lewis and his group at CalTech. They are using an STM immersed in water. The aqueous environment is most suitable for the study of hole creation. The threshold voltages, the depth of the holes and the size of the holes are more reproducible as compared to the uncontrolled environment of atmospheric air.

4. Gold on Gold Epitaxy

These studies were performed using a pocket-size ultra-high vacuum STM with exchangeable tips and samples in a chamber equipped with sample preparation facilities for sputtering, annealing and evaporation. Gold substrates were grown epitaxially on mica in a separate preparation chamber at the Ginzton Microfabrication Laboratory.

Characteristic of the initial stages of nucleation in the silver-gold system is single layer clustering, with island geometries determined by the particular overlayer-substrate metal combination. Since gold, in contrast to silver, is the only fcc(111) surface known to reconstruct, the role of the presence, removal or absence of a substrate reconstruction for the growth behavior could be studied in detail.

Finally, a study of ion bombarded Au(111) surfaces revealed the first images of the initial and progressing stages of sputtering damage. Both the energy-dependent sputtering yield and hole size distributions could be quantitatively characterized using STM. On the atomic scale, a fascinating duality between surfaces modified by deposition of atoms (evaporation) and vacancies (sputtering) was discovered.

C. DISCUSSION

1. Integrated Systems (STM-on-a-chip, the AFM)

The AFM, with a capability of imaging insulating as well as conductive surfaces, requires a scheme for detecting motion of the cantilever in the sub-angstrom range. The detection schemes now in use center on optical methods for detecting the motion. These systems are difficult to build and hard to operate because the optical components require

28

very fine alignments. In the alternative detection scheme proposed microfabrication techniques are used to define a piezoresistor on the cantilever, itself. As the cantilever is deflected the value of the resistor changes. This integrated system where monitors sense the motion of the cantilever without external monitoring systems will simplify the design and operation of the atomic force microscope.

2. AFM Studies

(a) VLSI Metrology with the AFM

The AFM clearly improves upon conventional micron-scale dimensional measurement instruments in several areas. It provides true height information about the sample without the low resolution, slow speed, single line-traces of a stylus profilometer. It provides the high resolution, real-time imaging capabilities of an SEM without requiring that the sample be conducting or be put in vacuum. For these reasons, the AFM has promise as a useful dimensional measurement instrument. Several key areas of the AFM still need improvement, however. The scan range of 18 μm is at the lower limit of a being useful for these applications. It needs to be improved to 50-100 μm to simplify use of the instrument. Coupling such a long-range scanner with an optical microscope and a translation stage for precision placement of the tip on the area of interest would greatly improve the microscope's utility. The other major problem with the scanner is a significant non-linearity. The accuracy of measurements are only as good as the accuracy of the scanner. Currently, the scanner is plagued by hysteresis, creep, and non-linear extension. These problems can make measurement errors as large as 25%. We are studying these non-ideal characteristics of the scanner by imaging regular arrays of dots that have a period of 1500 Å. These images give a quantitative measure of scanner non-linearities. We are examining several methods for eliminating the problems: open-loop drive signal correction, controlling the charge on the piezoelectric rather than the voltage, and closed-loop scan correction.

The other component of the microscope that still needs improvement is the tip. While vast improvements have been made in microfabricating integral sharp tips onto cantilever beams, significant tip artifacts still appear in images of structures with tall features. Currently, the apex angle of our tips is approximately 37°. Narrowing this angle would improve the imaging characteristics of the tip at the cost of making it more fragile. Since the tips are currently quite rugged, we hope to design tips with a narrower apex angle in order to find the optimal shape.

(b) Charge storage

The charge storage method that we have demonstrated appears to be one of the more promising techniques for data storage using an STM or AFM. The information may be erased and rewritten many times and the data rate is only limited by the fly-height of the cantilever over the surface and the noise of the capacitive sensor. These limitations are much more forgiving than the atomic-scale feedback required for reliable STM scanning. We have already demonstrated a storage density of 2 Gbit/cm^2. We hope to improve this by making sharper and more rugged tips and increasing the sensitivity of our capacitive sensor.

There are many other applications for a capacitance microscope using a flexible cantilever beam as a probe, such as laterally-resolved doping profile measurements and accurate measurements of insulating film thicknesses and uniformity. We hope to explore these and other applications of this instrument in the future.

3. Nanometer-Scale Hole Formation on Graphite using an STM

Chemical erosion of graphite in the presence of water vapor has a rich literature. Chemical erosion of surfaces proceeds with atoms in the lattice reacting with particles, such as molecules or ions, incident on the surface or adsorbed on the surface. The new species that result from this reaction have a smaller binding energy and desorb from the surface leaving a vacancy at the site where the surface atom was removed.

Chang and Bard[2] have used the STM to study the etch pits formed by heating graphite in air to 650°C for several minutes. They found that the pits formed with this termal process were identical in size and depth to those formed with electron enhanced etching.

The chemical nature of the molecules desorbed by the chemical erosion of carbon has been studied by Ashby and Rye.[3] The authors were interested in the design of reactors and the deterioration of graphite used as moderators. In their studies they bombarded the graphite surface with atomic hydrogen. They monitored the desorbed species with a mass spectrometer and found that the major component was methane (CH_4). They found a "major reactivity enhancement" when the surface was simultaneously bombarded with electrons. The rate of methane production was increased by a factor of twenty.

Their finding is consistent with earlier work by Hennig and Monet[4] where they determined that single vacancies were created in perfect layers when they irradiated these surfaces with electrons with energies in the range of 0.14 to 0.26 keV. It is, also, consistent with the studies of etching processes in the TEM.

In the TEM a carbon film is often used as a support for the specimens. It is a common experience to find that these films are 'etched' in the region covered by the electron beam. In one model it is assumed that the water molecules adsorbed on the film are ionized with electron beam. This increases their reactivity to the point where they can react with the carbon to form CO; the volatile product that is removed. The carbon support is thinned in the region of the e-beam. Original work on this system is contained in the paper by Egerton and Roussouw.[5]

'Electron enhanced etching' of graphite with tunneling current in the STM has been reported by several groups. Albrecht et al.[6] reported (included in our 1989 report) that the graphite surface can be etched with a single pulse on the tip of the STM operating in air with high relative humidity. The pits were formed by pulsing the tip to 5 volts for a few microseconds. The size and shape were identical to those observed by Chang and Bard in their thermal etching system. Terashima et al.[7] found similar results in their work on

surface modification. Mizutani et al.[8] have shown us how to use this process to scribe structures with a special shape in the uppermost layer of graphite. They positioned the tip at successive points along the circumference of a circle 100 Å in diameter. At each point they pulsed the tip voltage to form small pits overlapping to form a circular ditch around the circumference. The monolayer disk inside the circle was exfoliated leaving a circular hole conforming to the scribed outline.

More recent work has been reported by Penner et al.[9] They worked with a water immersion instrument. With pulses of 20 μs of 4 V on the tip they formed domes, rather than pits, on the graphite surface. The domes were 7 Å in diameter and 1 Å high. The domes were converted into the monolayer pits 30-40 Å in diameter by positioning the tip over the dome and pulsing the tip to 200 mV. The moderate voltage for conversion suggests that the domes are metastable intermediates in the path to the formation of pits.

4. Gold on Gold Epitaxy

These studies established STM as a unique tool for addressing issues in thin film growth on metal surfaces. The techniques employed for quantitative characterization proved widely applicable. There seems ample opportunity for further STM studies of on-metal systems, including the technologically interesting case of magnetic thin films.

REFERENCES

1. J.J. Chang, "Non-Volatile Semiconductor Memory Devices", Proc. IEEE **64**, 1039-1059 (1976).

2. H. Chang and A.J. Bard, "Formation of Monolayer Pits of Controlled Nanometer Size on Highly Oriented Pyrolytic Graphite by Gasification Reactions as Studied by Scanning Tunneling Microscopy", *J. Am. Chem. Soc.* **112**, 4598-4599 (1990).

3. C.I.H. Ashby and R.R. Rye, "Electron Enhanced Hydrogen Attack on First Wall Materials", *J. Nucl. Mater.* **103/104**, 489-492 (1981).

4. G.R. Hennig, "Electron Microscopy of Reactivity Changes near Lattice Defects in Graphite", p. 1-49, *in* Chemistry and Physics of Carbon, vol. 2, P.L. Walker, Jr., Editor, Marcel Dekker, Inc., New York (1966); also, R.T. Yang, "Etch-Decoration Electron Microscopy Studies of the Gas-Carbon Reactions", p. 163-210, *in* Chemistry and Physics of Carbon, vol. 19, P.A. Thrower, Editor, Marcel Dekker, Inc., New York (1984).

5. R.F. Egerton and C.J. Roussouw, "Direct Measurement of Contamination and Etching Rates in an Electron beam", *J. Phys. D: Appl. Phys.* **9**, 659-663 (1976).

6. T.R. Albrecht, M.M. Dovek, M.D. Kirk, C.A. Lang and C.F. Quate, "Nanometer-Scale Hole Formation on Graphite using A Scanning Tunneling Microscope", *Appl. Phys. Lett.* **55**, 1727-1729 (23 October 1989);

7. K. Terashima, M. Kondoh and T. Yoshida, "Fabrication of Nucleation Sites for Nanometer Size Selective Deposition by Scanning Tunneling Microscope", *J. Vac. Sci. Technol. A* **8**, 581-584 (Jan/Feb 1990).

8. W. Mizutani, J. Inukai and M. Ono, "Making a Monolayer Hole in a Graphite Surface by Means of a Scanning Tunneling Microscope", *Jap. J. Appl. Phys.* **29**, L815-L817 (May 1990).

9. R.M. Penner, M.J. Heben, N.S. Lewis and C.F. Quate, "Mechanistic Investigations of STM Lithography at Liquid-Covered Graphite Surfaces", to be published.

D. <u>PUBLICATIONS CITING JSEP SPONSORSHIP</u>
    (Partial Support)

(1) C.A. Lang, M.M. Dovek, J. Nogami, and C.F. Quate, "Au(111) autoepitaxy studied by scanning tunneling microscopy," *Surface Science*, **224**, L947-L955 (1989).

(2)   M.M. Dovek, C.A. Lang, J. Nogami, and C.F. Quate, "Epitaxial growth of Ag on Au(111) studied by scanning tunneling microscopy," *Phys. Rev. B*, **40**, 11973-11975 (1989).

Device Related Properties of High-temperature Superconductors

A. Kapitulnik
(415) 723-3847

A.   INTRODUCTION

We have developed methods to study some properties of high-temperature superconductors as related to device applications. In particular we rely on our ability to grow unique single crystals of $Bi_2Sr_2CaCu_2O_{8+\delta}$. These crystals, that are of very high purity and exhibit very low pinning were exclusively developed under JSEP sponsorship. We have divided our work into two parts. The first is the feasibility of a proximity effect between a high-temperature superconductor and a normal metal. Here we have been using photoemission technique to study the density of states at the Fermi level with metal deposited on the freshly cleaved superconductor. The second part is the development of a photothermal method for studying the thermal properties of the superconductor and in particular to image the superconductor as current is applied through the sample. As an example this method is a way to scan on a gross scale the critical current distribution in striplines of high-temperature superconductors.

B.   SUMMARY OF PRINCIPAL ACCOMPLISHMENTS

1. We have developed a directional solidification method for growing large single crystals in the $Bi_2Sr_2CaCu_2O_{8+\delta}$ system with excellent superconducting properties. We have recently improved our method by using MgO crucibles.

2. We have studied the magnetic properties of the crystals. We have shown that the crystals have very little pinning, a fact that allow us to study pinning effects and the behavior of the mixed state with progression of pinning density. (This work is done in collaboration with A. Leone at Lockheed, who is doing the proton and neutron irradiation of the crystals).

35

3. Using photoemission, we have shown that the crystals cleave at the Bi-O layer by studying the valance bands of Rb deposited freshly cleaved crystals.

4. We have studied Au deposited on the ab plane of a freshly cleaved crystal. A well pronounced superconducting gap was observed on the bare surface but no proximity effcet was detected.

5. We have observed for the first time the existence of a Hexatic phase of the flux lattice that separates the solid and liquid phases.

6. We have measured for the first time the optical anisotropy of $Bi_2Sr_2CaCu_2O_8$ crystals. We have shown that they behave like insulators along the c direction.

C.   DISCUSSION

To study the proximity effect, high quality surfaces of the HTSC are required. Of all HTSC, only in the $Bi_2Sr_2CaCu_2O_{8+\delta}$ system we can achieve high quality surface by cleaving the crystal in between two successiveBi-O layers. Thus, we have developed a directional solidification method for growing large single crystals in the $Bi_2Sr_2CaCu_2O_{8+d}$ system with excellent superconducting properties. Annealing the crystals in increasing partial pressures of oxygen reversibly depresses the superconducting transition temperature from 90K (as made) to 70K (oxygen high pressure annealed) while the carrier concentrations as determined from Hall effect measurements, increase from n = $3.1(3)x10^{21}$ cm^{-3} (0.34 holes/Cu site) to $4.6(3)x10^{21}$ cm^{-3} (0.50 holes/Cu site).

The crystals have been used for many measurements like transport, thermal conductivity, heat capacity and optical properties. Of particular importance for the understanding of proximity effects are the tunneling (discussed in our previos report) and photoemission measurements performed on the crystals. Using deposition of Rb on the freshly cleaved surface we have shown undoubtedly for the first time that indeed the crystal cleaves at the Bi-O layer. We further showed, using LEED and STM (with Prof. Quate) that the previously observed superstructure in the ab plane is commensurate with the crystal and arises from the mismatch between the Cu-O and the Bi-O bonds. This was the first STM study with atomic resolution in the field of HTSC.

Using high resolution angle resolved photoemission measurements, we have studied the Fermi surface and how it changes with doping. The Fermi surface consists of two distinct pieces. The first is Cu-O derived bands cutting the Fermi level in the Γ-X and Γ-Y directions and the second is a pocket derived principally from Bi-O states around the Γ-M point in the Brillouin zone. In all three directions a gap was observed as the temperature was lowered below the superconducting transition temperature. To study proximity effect, we have studied the spectra from gold covered freshly cleaved crystals. To test the idea that destroying the superconductivity in the Bi-O layer does not affect the superconductivity in the Cu-O layers, we have deposited submonolayer of gold on the (Bi-O plane as discussed above) cleaved crystal. Indeed, the gap structure was destroyed only along the Γ-M direction. We further deposited more gold to check for proximity effect. We have found no gap structure along any direction although the gold character was already metallic. We thus concluded that no proximity effect is possible between gold and BiSrCaCuO crystals alog the c-axis. This result is not surprising since the c-axis coherence length is shorter than the interlayers distance. Moreover, because of the two-dimensional character of this system, it is hard for electrons to change momentum from in-plane to out of plane direction. An inelastic process that destroys the coherence and thus the proximity effcet is the only possible way for such a process. Evidently, we need to study further the proximity effect along the c direction where the coherence length is longer.

To study the thermal properties of the high-Tc materials we have developed a photothermal method (with Prof. Kino) that is capable in looking at variations in thermal properties of the material with ~2μm spatial resolution. In this technique the sample is heated periodically by a modulated argon-ion laser beam and the resulting periodically varying temperature profile is measured by using a second diode laser. Both beams are focused with a microscope objective, so the resolution of the measurement is determined by the diffraction limited spot size of the laser beams. The temperature is measured by exploiting either the change in refractive index with temperature or the change in the slope of the sample surface due to thermal expansion. The delay in the response between the excitation beam and the probe beam causes a phase lag that is proportional to the thermaldiffusivity and to the square root of the modulation frequency. Using this photothermal technique, we have measured for the first time the anisotropy in the thermal conductivity of $Bi_2Sr_2CaCu_2O_{8+\delta}$ crystals and more recently as a function of temperature. We were the first to note that electron-phonon interaction is pronounced in the Cu-O planes but almost does not exist in the perpendicular direction. But, of the most important discoveries using this method was its ability to discriminate "good" and "bad" regions on a

macroscopic scale (as they have different thermal properties). To enhance this effect we are not using the phase shift of the thermal signal but rather the amplitude as observed by the probe beam. In this configuration, a much tighter arrangement can be used (e.g. the two beams overlap) and thus a scale of ~1μm can be reached. The source of the amplitude signal is not understood yet and is being studied by us. This method is thus of particular interest to evaluate the current distribution as we exceed the critical current in thin films and thin films devices. The length scale of ~1μm is of particular interest as it is of a typical size of devices or natural grain sizes.

Recently, we built a completely new system that is UHV and thus less susceptible to surface contamination. We added an autofocus device such that the system can measure automatically even if focus is momentarily lost because of thermal drift or, more importantly, due to scanning the sample. This last feature is very important if we want to scan large areas using the thermal probe. We also added to the system an in-situ susceptometer that can measure the shielding response simoultanously with the thermal measurement. This addition is important to correlate the onset of superconductivity with the appearance of thermal signals.

D.   PUBLICATIONS CITING JSEP SPONSORSHIP

1.   Mitzi, D.B., L.W. Lombardo, A. Kapitulnik, S.S. Laderman and R.D. Jacowitz, "Growth and properties of oxygen and ion doped $Bi_2Sr_2CaCu_2O_{8+\delta}$ single crystals," *Phys. Rev.* **B 41** (1990), 6564.

2.   KIm, J.H., I. Bozovic, D.B. Mitzi, A. Kapitulnik and J.S. Harris Jr., "Optical Anisotropy of $Bi_2Sr_2CaCu_2O_8$," *Phys. Rev.* **B 41** (1990), 7251.

3.   Murray, C.A., P.L. Gammel, D.J. Bishop, D.B. Mitzi and A. Kapitulnik, "Observation of a Hexatic Vortex Glass in Flux Lattices of the High-Tc Superconductor $Bi_{2.1}Sr_{1.9}Ca_{0.9}Cu_2O_{8+\delta}$," *Phys. Rev. Lett.* **64** (1990), 2312.

4.   Wells, B.O., Z.-X Shen, D.S. Dessau, W.E. Spicer, C.G. Olson, D.B. Mitzi, A. Kapitulnik, R.S. List and A. Arko, "An Angle Resolved Photoemission Study of $Bi_2Sr_2CaCu_2O_{8+\delta}$ with Varied Oxygen Content: Metallicity of the Bi-O Plane," to be published in *Phys. Rev. Lett.* (1990).

5. Dessau, D.S., R.S. List, Z.X-. Shen, A.J. Arko, R.J. Bartlett, B.O. Wells, D.B. Mitzi, L. Lombardo, Z. Fisk, S-.W. Cheong, J.E. Schriber, A. Kapitulnik, I. Lindau and W.E. Spicer, "Electronic structure of the Gold/$Bi_2Sr_2CaCu_2O_8$ and Gold/$EuBa_2Cu_3O_{7-\delta}$ Interface as Studied by Photoemission Spectroscopy, Submitted to *Appl. Phys. Lett.*

Appendix

Biography of Principal Investigators

1. David M. Bloom

David M. Bloom was born on 10 October 1948 in Brooklyn, NY. He received the B.S. degree in electrical engineering from the University of California Santa Barbara in 1970 and the M.S. and the Ph.D. degrees in electrical engineering from Stanford University in 1972 and 1975, respectively.

From 1975 to 1977 he was employed by Stanford University as a Research Associate. During this period he was awarded the IBM Postdoctoral Fellowship. From 1977 to 1979 he was employed by Bell Telephone Laboratories, Holmdel, NJ., where he conducted research on optical phase conjugation, ultrafast optical pulse propagation in fibers, and tunable-color-center lasers. From 1979 to 1983 he served on the staff and later as a Project Manager at Hewlett-Packard Laboratories, Palo Alto, CA. While there he conducted and managed research on fiber optical devices, high-speed photodetectors, and picosecond electronic measurement techniques. In late 1983 he joined the Edward L. Ginzton Laboratory, W. W. Hansen Laboratories of Physics, Stanford University, where he is currently an Associate Professor of Electrical Engineering. His current research interests are ultrafast optics and electronics.

He was awarded the 1980 Adolph Lomb Medal of the Optical Society of America for his pioneering work on the use of nonlinear optical processes to achieve real time conjugate wavefront generation. In 1981 he was elected a Fellow of the Optical Society of America in recognition of his distinguished service in the advancement of optics. He was the 1985 IEEE LEOS traveling lecturer. In 1986 he was elected a Fellow of the Institute of Electrical and Electronics Engineers for contributions to nonlinear optics and ultrafast optoelectronics.

2. Robert L. Byer

Professor Byer received his Ph.D. in 1969 in Applied Physics at Stanford University. His early work led to ther first observation of optical parametric fluorescence and to the first demonstration of CW optical parametric oscillation in $LiNbO_3$.

After joining the Applied Physics Department in 1969, Professor Byer initiated research in remote sensing using tunable laser sources. Research in that area led to the development of the unstable resonator Nd:YAG laser and to high power tunable infrared generation in $LiNbO_3$ parametric tuners.

In 1974 Professor Byer and his colleagues initiated research in Coherent Anti-Stokes Raman Spectroscopy (CARS), named the effect, and continued research on high resolution Raman spectroscopy in pulsed and supersonic nozzle expansions.

In 1976 Professor Byer suggested the use of stimulated Raman scattering in hydrogen gas to generate $16\mu m$ radiation from a CO_2 laser source. Research at Stanford University confirmed the expected simplicity and efficiency of the approach.

In 1980 research on slab geometry solid state lasers was begun. The program led to the successful theoretical and experimental development of high peak and average power solid state laser sources. Research in advanced solid state laser sources is continuing with emphasis on laser-plasma produced soft X-ray radiation for application to X-ray microscopy and X-ray lithography.

Current research interests include the study of laser diode pumped miniature solid state laser sources, the growth and application of single crystal fibers, and the synthesis of advanced nonlinear materials.

Professor Byer is a Fellow of the Optical Society of America, a Fellow of the Institute of Electrical and Electronics Engineers, a Member of the American Physical Society and the American Association for the Advancement of Science. In 1985 Professor Byer was President of the IEEE Lasers and Electro-optics Society. He was Chairman of the Applied Physics Department from 1981 to 1984 and was appointed Associate Dean of Humanities and Sciences in 1985. In 1987 he was appointed Vice Provost and Dean of Research.

He has worked in industry at Spectra Physics (1964-65), and has consulted for numerous companies including Chromatix, Molectron, Westinghouse, General Motors, Newport and Hoya. He was co-founder of Quanta Ray Inc. in 1975, and of Lightwave Electronics Corp. in 1984.

Professor Byer has published more than 170 scientific papers and holds 15 patents in the field of nonlinear optics and laser devices.

3. C. F. Quate

B.S. (1944) University of Utah; Ph.D. (1950) Stanford University. Bell Laboratories (1949-58). Sandia Corporation (1959-61). Guggenheim Fellow and Fullbright Scholar, Faculte des Sciences, Montpellier, France (1968-69). At Stanford University since 1961; Chairman, Department of Applied Physics (1969-72; 1978-81); Associate Dean, School of Humanities and Sciences (1972-74; 1982-83); first Leland T. Edwards Professor of Engineering (1986--). Senior Research Fellow, Xerox Palo Alto Research Center (PARC) since July 1984. Member: National Academy of Engineering; National Academy of Sciences; American Physical Society; Institute of Electrical and Electronics Engineers (Fellow); American Academy of Arts and Sciences (Fellow); Acoustical Society (Fellow); Royal Microscopical Society (Honorary Fellow). Awarded the IEEE Morris N. Liebman Award (1981); Rank Prize for Opto-electronics (1982); IEEE Achievement Award Ultrasonics; Ferroelectrics and Frequency Control Society (1986); IEEE Medal of Honor (1988).

Research interests include linear properties of acoustic waves in the microwave region. Imaging, scanning microscopy and new concepts for data storage. This includes both acoustic waves and vacuum tunneling.

Holder/co-holder of 42 patents.
Author/co-author of over 150 publications.

4. Aharon Kapitulnik

Aharon Kapitulnik was born in Tel Aviv, Israel on July 29, 1953. He received his B.Sc. in 1978, and his Ph.D. in 1984, both from Tel Aviv University.

In 1983 and 1984 he held the Chaim Weizman Postdoctoral Fellowship at the Institute for Polymers and Organic Solids at the University of California at Santa Barbara. In 1985 he was an Assistant Professor in the Department of Physics at UC Santa Barbara, then Member of the Center for Materials Research at Stanford University. He was also awarded an IBM Faculty Development Award for 1985-1987. In 1986 he was awarded an Alfred P. Sloan Fellowship, and in 1987 and 1988 the Presidential Young Investigator Award. In 1988 he was awarded the 1987 Bergman Memorial Research Grant by the USA-Israel BSF. Since 1985, Dr. Kapitulnik has been an Assistant Professor in the Department of Applied Physics at Stanford University.

5. Stephen E. Harris

Stephen E. Harris was born in November 1936 in Brooklyn, New York. He received the B.S. degree in electrical engineering from Rensselaer Polytechnic Institute in 1959. After one year at Bell Telephone Laboratories, he attended Stanford University where he received the M.S. and Ph.D. degrees in electrical engineering in 1961 and 1963, respectively. Since 1963 he has been on the faculty of Stanford University where he is now a Professor of Electrical Engineering and of Applied Physics. His research work has been in the fields of lasers, quantum electronics, nonlinear optics, and atomic physics. His present research interests are in the areas of new techniques for generating extreme ultraviolet and soft x-ray radiation.

Professor Harris was the recipient of the 1973 Curtis McGraw Research Award, the 1978 David Sarnoff Award, the 1984 Clarence Davies Medal, and the 1985 Charles Hard Townes Award. He is a Fellow of the IEEE, the Optical Society of America, and the American Physical Society. In 1977 he was elected to the National Academy of Engineering, and in 1981 he was elected to the National Academy of Sciences. In 1988 he was named as the Kenneth and Barbara Oshman Professor of Engineering.

DD147

REPORT DOCUMENTATION PAGE

1a. REPORT SECURITY CLASSIFICATION Unclassified	1b. RESTRICTIVE MARKINGS
2a. SECURITY CLASSIFICATION AUTHORITY 2b. DECLASSIFICATION/DOWNGRADING SCHEDULE	3. DISTRIBUTION/AVAILABILITY OF REPORT Approved for public release: distribution unlimited

4. PERFORMING ORGANIZATION REPORT NUMBER(S) GL 4738	5. MONITORING ORGANIZATION REPORT NUMBER(S)

6a. NAME OF PERFORMING ORGANIZATION Edward L. Ginzton Laboratory Stanford University	6b. OFFICE SYMBOL Code: 2E254	7a. NAME OF MONITORING ORGANIZATION Office of Naval Research (for) Joint Services Electronics Program
6c. ADDRESS (City, State and ZIP Code) Stanford University Stanford, California 94305		7b. ADDRESS (City, State and ZIP Code) 800 North Quincy Street Arlington VA 22217-5000

8a. FUNDING/SPONSORING ORGANIZATION Joint Services Electronics Program	8b. OFFICE SYMBOL	9. PROCUREMENT INSTRUMENT IDENTIFICATION NUMBER N00014-84-K-0327

8c. ADDRESS (City, State and ZIP Code) Dr. Kristal Hathaway (414) Head, Electronics Division Office of Naval Research 800 North Quincy Street Arlington, VA 22217-5000	10. SOURCE OF FUNDING NOS.

PROGRAM ELEMENT	PROJECT NO.	TASK NO.	WORK UNIT NO.

11. TITLE
ANNUAL PROGRESS REPORT: JSEP CONTRACT N00014-84K-0327 for the period ending 9 September 1990

12. PERSONAL AUTHORS
S.E. HARRIS, D.M. Bloom, R.L. Byer, C.F. Quate and A. Kapitulnik

13a. TYPE OF REPORT Annual Progress Report	13b. TIME COVERED 10 Oct 89 – 9 Oct 90	14. DATE OF REPORT (Yr Mo Day) 90 10/09	15. PAGE COUNT 44

16. SUPPLEMENTARY NOTATION The views, opinions and/or findings contained in this report are those of the authors and should not be construed as an official Dept of Defense position, policy or decision unless otherwise documented.

17. COSATI CODES			18. SUBJECT TERMS (Continue on reverse if necessary & identify by block no.
FIELD	GROUP	SUB GROUP	

19. ABSTRACT (Continue on reverse if necessary & identify by block no.)

Annual Progress Report for JSEP Contract N00014-84-K-0327 for the period 10 OCT 89-9 SEP 90. Projects are: UNIT 90-1 Development of an all-silicon integrated optical modulator for high speed data communications (D.M. Bloom); UNIT 90-2 Synthetic nonlinear media (R.L. Byer); UNIT 90-3 Scanning tunneling microscopy (C.F. Quate); UNIT 90-4 Device related properties of high temperature superconductors (A. Kapitulnik).

20. DISTRIBUTION/AVAILABILITY OF ABSTRACT UNCLASSIFIED/UNLIMITED [X] SAME AS RPT [] OTIC USERS []	21. ABSTRACT SECURITY CLASSIFICATION Unclassified

22a. NAME OF RESPONSIBLE INDIVIDUAL S.E. HARRIS, JSEP Program Director, Ginzton Laboratory	22b. TELEPHONE NUMBER (415) 723-0224	22c. OFFICE SYMBOL

REPORT DOCUMENTATION PAGE (CONTINUATION)

18. SUBJECT TERMS (Continued)

19. ABSTRACT (Continued)